

Enhanced development of a catalyst chamber for the decomposition of up to 1.0 kg/s hydrogen peroxide

Ognjan Božić¹ · Dennis Porrman¹ · Daniel Lancelle¹ · Stefan May¹

Received: 16 December 2014 / Revised: 20 November 2015 / Accepted: 21 November 2015 / Published online: 12 December 2015
© CEAS 2015

Abstract A new innovative hybrid rocket engine concept is developed within the AHRES program of the German Aerospace Center (DLR). This rocket engine based on hydroxyl-terminated polybutadiene (HTPB) with metallic additives as solid fuel and high test peroxide (HTP) as liquid oxidizer. Instead of a conventional ignition system, a catalyst chamber with a silver mesh catalyst is designed to decompose the HTP. The newly modified catalyst chamber is able to decompose up to 1.0 kg/s of 87.5 wt% HTP. Used as a monopropellant thruster, this equals an average thrust of 1600 N. The catalyst chamber is designed using the self-developed software tool SHAKIRA. The applied kinetic law, which determines catalytic decomposition of HTP within the catalyst chamber, is given and commented. Several calculations are carried out to determine the appropriate geometry for complete decomposition with a minimum of catalyst material. A number of tests under steady state conditions are carried out, using 87.5 wt% HTP with different flow rates and a constant amount of catalyst material. To verify the decomposition, the temperature is measured and compared with the theoretical

prediction. The experimental results show good agreement with the results generated by the design tool. The developed catalyst chamber provides a simple, reliable ignition system for hybrid rocket propulsion systems based on hydrogen peroxide as oxidizer. This system is capable for multiple reignition. The developed hardware and software can be used to design full scale monopropellant thrusters based on HTP and catalyst chambers for hybrid rocket engines.

Keywords Hydrogen peroxide · Catalyst chamber · Hybrid rocket engine · Monopropellant thruster

Abbreviations

AHRES	Advanced Hybrid Rocket Engine Simulation
H ₂ O	Water
H ₂ O ₂	Hydrogen peroxide
O ₂	Oxygen
HRE	Hybrid rocket engine
HTPB	Hydroxyl-terminated polybutadiene
HTP	High test peroxide
LRE	Liquid rocket engine
NTO	Dinitrogen tetroxide (N ₂ O ₄)
SHAKIRA	Simulation of High test peroxide Advanced (K)catalytic Ignition system for Rocket Applications

List of symbols

A_0 [mol/(s·kg _{cat} ·K ^{1/2})]	Zero order reaction const
A_1 [m ³ /(s·kg _{cat} ·K ^{1/2})]	First order reaction const
c_p [J/(kg K)]	Specific heat capacity at constant pressure
c_v [J/(kg K)]	Specific heat capacity at constant volume

This paper is based on a presentation at the 4th (International) Space Propulsion Conference, May 19–22, 2014, Cologne, Germany.

✉ Ognjan Božić
ognjan.bozic@dlr.de

Dennis Porrman
dennis.porrman@dlr.de

Daniel Lancelle
daniel.lancelle@dlr.de

Stefan May
stefan.may@dlr.de

¹ German Aerospace Center (DLR), Institute of Aerodynamics and Flow Technology, Braunschweig, Germany

c^* [m/s]	Characteristic velocity
E_a [J/mol]	Activation energy
m [kg]	Mass
\dot{m} [kg/s]	Mass flow
M [kg/mol]	Molar mass
p_c [bar]	Catalyst chamber pressure
r [kg/s]	Decomposition rate
R [J/(K·mol)]	Universal gas const
R_i [J/(kg K)]	Specific gas const
T [K]	Temperature
x	Vapor fraction

Greek symbols

Γ	Vandenkerckhove function
Δp [bar]	Pressure drop
ΔT [K]	Temperature difference
$\eta_{\Delta T}$	Temperature efficiency
η_{c^*}	Characteristic velocity efficiency
κ	Heat capacity ratio
ρ [kg/m ³]	Density
τ	Process time interval
ω	Mass fraction

Subscripts

ad	Adiabatic
cat	Catalyst conditions
CB	Catalyst bed
env	Environmental
exp	Experimental value
FL	Feed line
H ₂ O ₂	Conditions of H ₂ O ₂
mean	Average value
max	Maximum value
theo	Theoretical value

1 Introduction

In the last 15 years, a number of companies, research institutions and universities worldwide have investigated catalytic properties and combustion properties of HTP and applied it to different rocket propulsion systems (e.g., Rocketdyne (USA), NASA—J. Stennis (USA), Purdue University—W. Lafayette (IN, USA), General Kinetics (CA, USA), Herakles—Safran (F), ONERA (F), DLR—AS Braunschweig (D); ALTA S.p.A., Pisa (I), University Road—Southampton (UK), Defence Agency for Technology—Seoul, (South Korea) as well as a number of universities and research institutions in China). Rocket engines based on HTP as oxidizer can be used for satellite propulsion (in mono- or liquid bi-propellant systems), as a thruster for LRE launcher boosters and HRE/LRE upper stages, moon landers, sounding rockets, rocket airplanes for

space tourism or for investigation of the upper Earth atmosphere layers. One additional HTP application recently investigated by several institutions in last time is a catalytic HTP ignition system for LRE and HRE, which represents a cheap and reliable solution. The use of HTP for hybrid rocket engines [1] has several positive aspects:

- A separate ignition system is not necessary,
- The structure/propellant mass ratio is lower than for other propellant mixtures,
- The regression rate of the solid fuel grain is higher compared to the large number of known propellant mixtures, which enables a higher thrust,
- The throttling of the engine can be efficiently realized by mass flow control of the HTP oxidizer, because the loss of specific impulse and performance is very low in broad range when the O/F ratio is shifting [1],
- The specific impulse for 92 % HTP-based propellant mixtures is equal or superior to corresponding mixtures with NTO and only 8 % lower than for corresponding mixtures with oxygen.
- By observing the basic rules of handling and HTP compliant design rules, the risk of fire, explosion or personal injuries is lower than for other high-energy propellant combinations.

These arguments delivered the basics for the start of the DLR program AHRES. This program includes the development and tests with a hybrid rocket engine demonstrator, based on HTPB with metallic additives as solid fuel and HTP as liquid oxidizer [1]. Instead of a conventional ignition system, a catalyst chamber with a silver mesh catalyst is designed to decompose the HTP to water vapor and oxygen at a very high temperature. The catalyst chamber is able to decompose currently up to 1.0 kg/s of 87.5 wt% HTP. Used as a monopropellant thruster, this results in a theoretical thrust of 1605 N at sea level. The preliminary test results achieved with this catalyst chamber are presented in this paper. With the self-developed DLR simulation code SHAKIRA (Simulation of High test peroxide Advanced K(C)atalytic Ignition system for Rocket Applications), the design of a catalyst chamber for decomposing HTP is carried out.

2 Simulation model

Within the 1 D simulation code SHAKIRA, the catalyst chamber is idealized as a hollow cylinder, which is discretized in axial direction. Calculations are carried out for each step in space, based on the results of the last step at steady state conditions. For the first step, initial conditions (medium temperature, pressure, mass concentration

of H_2O_2 , mass flow) are required. The conditions of the medium are assumed as ideal homogeneously in the volume of each step. SHAKIRA can be used to determine a lot of different catalytic materials and two different geometries (meshes and pebble beds) of the catalyst material itself. According to Pirault-Roy et al. [3], the catalytic decomposition of H_2O_2 shows a zero order or first order reaction character, depending on used catalytic material. In consequence, the developed decomposition model is designed for both kinds of reaction. The equation to determine the decomposition rate $r_{\text{H}_2\text{O}_2}$ is

$$r_{\text{H}_2\text{O}_2} = m_{\text{cat}} \cdot M_{\text{H}_2\text{O}_2} \cdot \left(A_0 + A_1 \cdot \omega_{\text{H}_2\text{O}_2} \cdot \frac{\rho_{\text{H}_2\text{O}_2}(T)}{M_{\text{H}_2\text{O}_2}} \right) \cdot \sqrt{T} \cdot \exp\left(-\frac{E_{a,\text{cat}}}{R \cdot T}\right) \quad (1)$$

with the molar mass $M_{\text{H}_2\text{O}_2}$, the effective catalyst mass m_{cat} , the zero order reaction factor A_0 , the first order reaction factor A_1 , the universal gas constant R and the catalytic material depending reaction activation energy $E_{a,\text{cat}}$. The temperature dependence of the reaction factors is approximated with the root of temperature as multiplier. The density of H_2O_2 consists of the liquid and the gaseous part:

$$\rho_{\text{H}_2\text{O}_2}(T) = \rho_{\text{H}_2\text{O}_2,l}(T) \cdot (1 - x_{\text{H}_2\text{O}_2}) + \rho_{\text{H}_2\text{O}_2,g}(T) \cdot x_{\text{H}_2\text{O}_2} \quad (2)$$

The effective catalytic mass m_{cat} depends on the geometry of the catalyst and therefore on the effective reacting surface. It describes the mass of the catalytic active surface for the discretized volume in each calculation step. To receive the reaction factors and the activation energy, experiments are necessary. Some experimental results are available in scientific publications [3–7]. The values for the silver meshes are determined with test information of the catalyst manufacturer “Preoxide Propulsion” (Sweden) [14]. A detailed description of the program code is given by May et al. [2]. The flowchart of SHAKIRA is shown in Fig. 1 to visualize the program logic.

In the predesign phase of the AHRES program, different options for the catalyst bed are determined (e.g., platinum-coated spheres, monolithic platinum based-catalyst, perovskite-based materials such as $\text{La}_{0,8}\text{Sr}_{0,2}\text{CoO}_3$ —referred as LSC). Due to the high costs of alternative catalyst materials and manufacturing complexity, in the first development step the catalytic chamber is equipped with silver meshes. They are easy to obtain, relatively cheap and have excellent advantages as a catalyst. In respect of his melting point, Silver is applicable for a concentration of up to 92 wt% H_2O_2 . Therefore, calculations with SHAKIRA for a chamber with a catalyst of mesh geometry and silver as catalytic material are carried out by a mass flow of 0.7 kg/s, an HTP concentration of 87.5 wt% and an

inner chamber diameter of 0.1 m. The simulation results are shown in Figs. 2 and 3. The evolution of the effective decomposition rate of H_2O_2 for each step and the evolution of media temperature are plotted in Fig. 2. Furthermore, the mass fractions of the three species H_2O_2 , H_2O and O_2 and the vapor fractions for H_2O_2 and H_2O are shown in Fig. 3. The vapor fractions are related to the phase condition of each single species and they are not linked with the fluid composition.

At first, the temperature and decomposition curves show a very flat progression and the decomposition rate is very low. After nearly 30 mm, the decomposition rate increases as a result of the significantly growing temperature. Past a short peak close to 42 mm, the decomposition rate decreases and the temperature stays at a plateau of almost 403 K. The reason for this behavior is that near to 42 mm of the chamber length the liquid mixture is starting to boil (see Fig. 3) and in that case, the average density of the medium and also the density of pure H_2O_2 significantly decrease. This means, the number of H_2O_2 molecules per volume is reduced. In respect to Eq. 1, the decomposition rate diminishes drastically. After about 56 mm, the whole medium is vaporized and the temperature is growing up again. Due to the exponential correlation between decomposition rate and medium temperature, the decomposition rate gains strongly. Thus, at nearly 65 mm, the whole H_2O_2 is completely decomposed into hot water vapor and oxygen.

In Fig. 4, the mass fractions of H_2O_2 vs. the distance from the inlet for a mass flow of 0.7, 1.0 and 1.3 kg/s are plotted. To ensure a complete decomposition of a mass flow up to 1.3 kg/s, the effective length of the designed catalyst chamber was chosen to be 0.13 m. The simulation shows clearly that such a mass flow could be completely decomposed within the designed catalyst chamber. In the current project step, the capacity of about 1.0 kg/s is tested. In forthcoming project steps, the maximum catalyst chamber capacity will be used.

3 Constructed catalyst chamber

Within the AHRES program the developed catalytic chamber is a modular robust solution which enables tests with different catalyst bed solutions for high HTP chamber pressures up to 70 bars. The presented design is primarily intended as pre-heated steam/gas generator with the aim to supply the discussed hybrid rocket engine demonstrator with gasified oxidizer and to enable multiple ignition of the engine without a separate ignition system. The established and proved catalyst chamber solution could also be upgraded to a HTP monopropellant thruster for different purposes, with moderate effort [8–10].

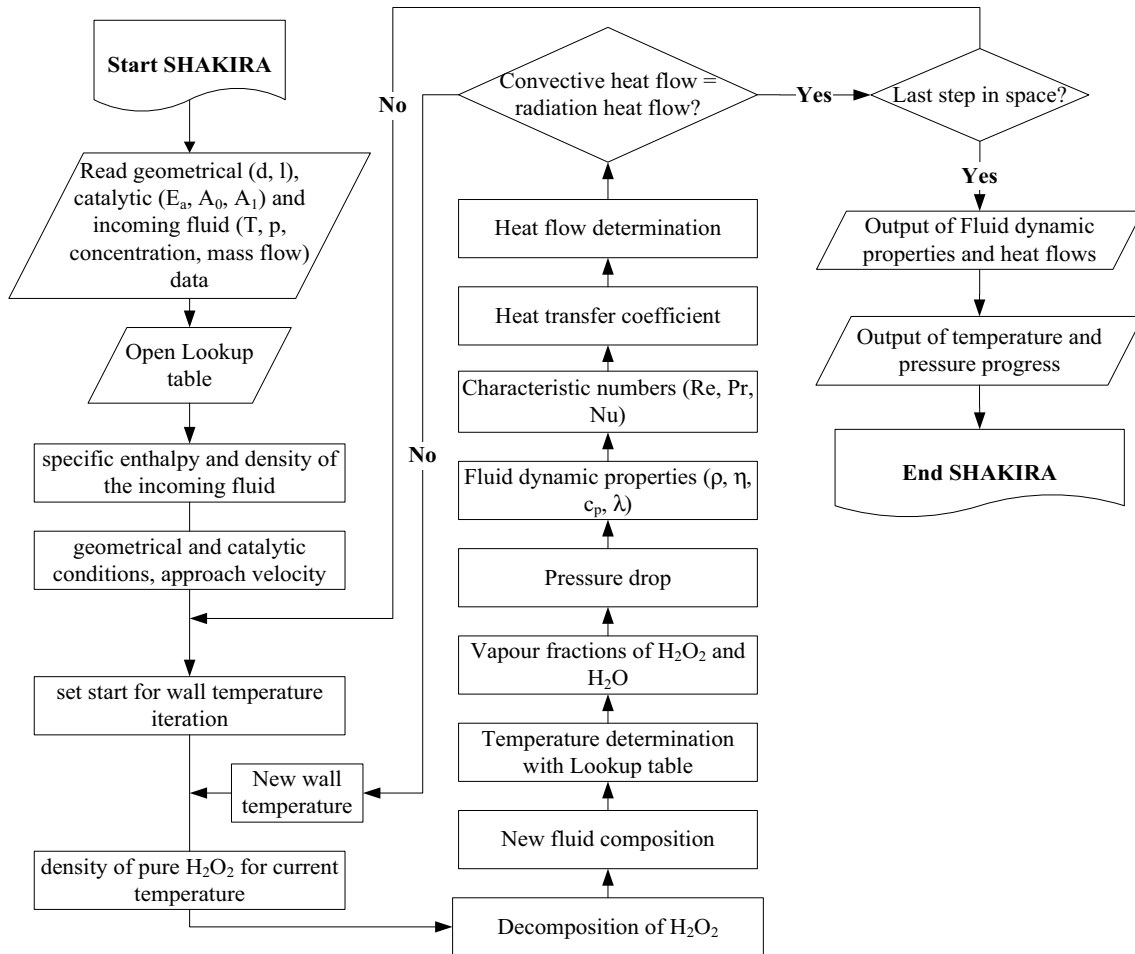


Fig. 1 Flowchart of the simulation program SHAKIRA

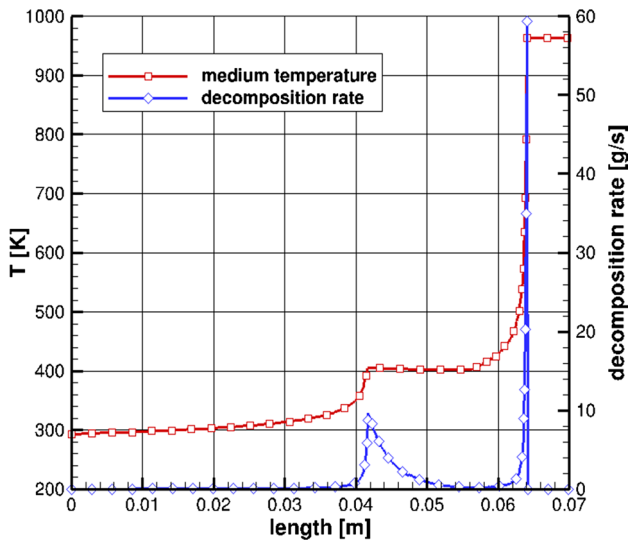


Fig. 2 Decomposition rate and medium temperature vs. length for a catalyst chamber with silver meshes and a mass flow of 0.7 kg/s [2]

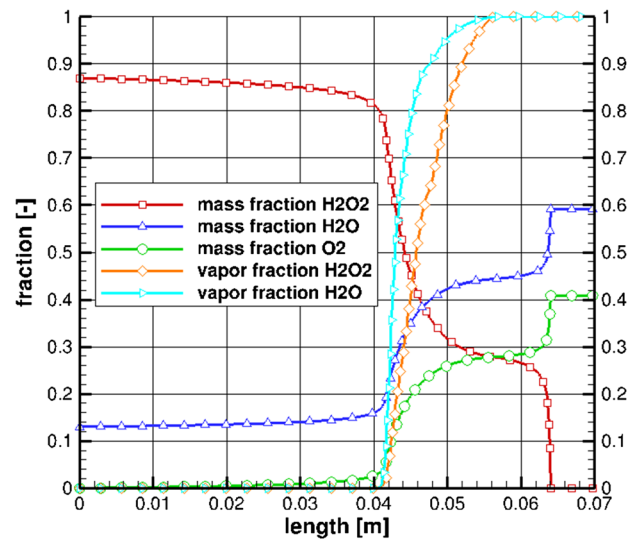


Fig. 3 Mass and vapor fractions for the three species H_2O_2 , H_2O and O_2 vs. length for a catalyst chamber with silver meshes and a mass flow of 0.7 kg/s [2]

The catalyst chamber housing is made up of Inconel 718 alloy to meet all future investigation requirements, which is rated for HTP concentrations up to 98 wt%. At the left and right ends of the housing, flange connectors are incorporated (s. Fig. 5) to enable a good sealing and more security for repeated connection/disconnection of design elements as is common during research activities. On the oxidizer inlet side (in direction of the HTP feeding line) a flat sealing gasket, made out of Teflon-based plastic, is mounted. To reduce the number of connection elements, which again reduces the security risks through bad sealing under dynamic operational conditions, the catalyst chamber is designed as mono-block construction with a combustion chamber injector in form of truncated cone for the HRE combustion chamber. The catalyst

mount, formed as cylindrical tube with an inner diameter of 100 mm, is inserted into the casing. It serves as mechanical protection for the catalyst bed. The catalyst bed consists of high purity silver meshes. Depending on the required HTP mass flow, up to 200 silver screens can be embedded within the catalyst mount. In current tests up to 172 catalyst silver screens are used. To prevent mesh deformation or break-up due to pressure pulses on the upper side (flow feeding side—oxidizer inlet), a mounting plate with integrated injector (Injector plate) is attached. Compared to former tests with the HRE (see Ref. [13]), this injector was modified to suppress pressure instabilities. On the bottom side, a support plate with a large number of holes is installed (mounting plate). Between the catalyst mounting and the catalyst chamber housing is a cylindrical gap. During the tests this gap contributes to the reduction of heat transfer to the housing. This reduces the ramp-up time until steady state working conditions are reached. The implemented design enables flexible handling with catalyst beds composed of heterogeneous structures or different catalyst materials. This is especially attractive for HTP applications with concentrations higher than 87.5 wt%.

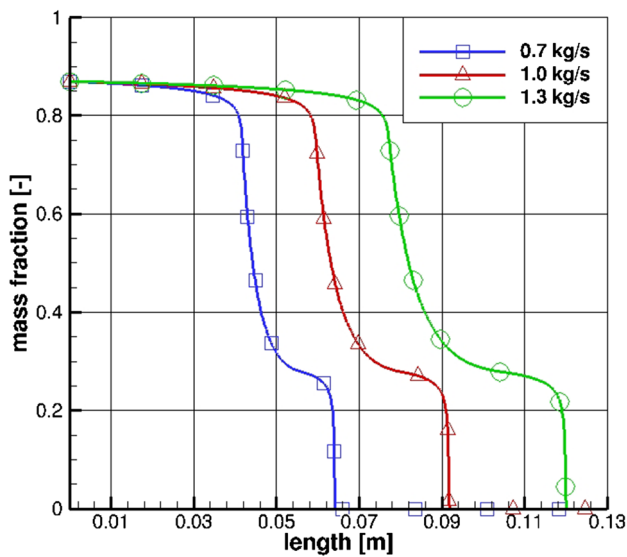


Fig. 4 Mass fractions of H_2O_2 vs. length for different mass flows

4 Description of the feed system

The main part of pressure feeding system of the oxidizer HTP is the high-pressure tank (s. Fig. 6). It is mounted on a stainless steel plate equipped with four force sensors, which enables the measurement of instantaneous HTP filling weight. As a redundant system, the filling level can be determined by means of an ultrasonic probe mounted at the base of the pressure vessel. The HTP tank is equipped with six flange connectors: four on the lateral side and one each on the top cover plate and the bottom tank side.

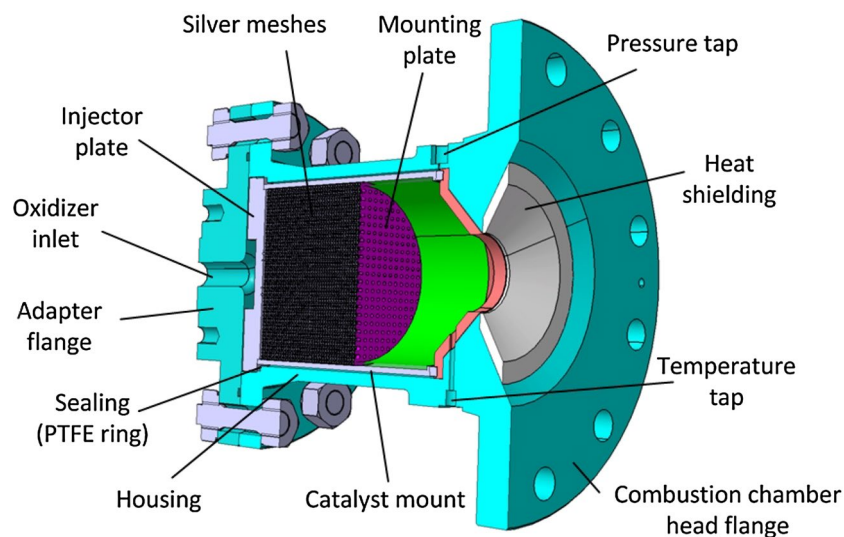


Fig. 5 Catalytic chamber for the AHRES hybrid rocket engine

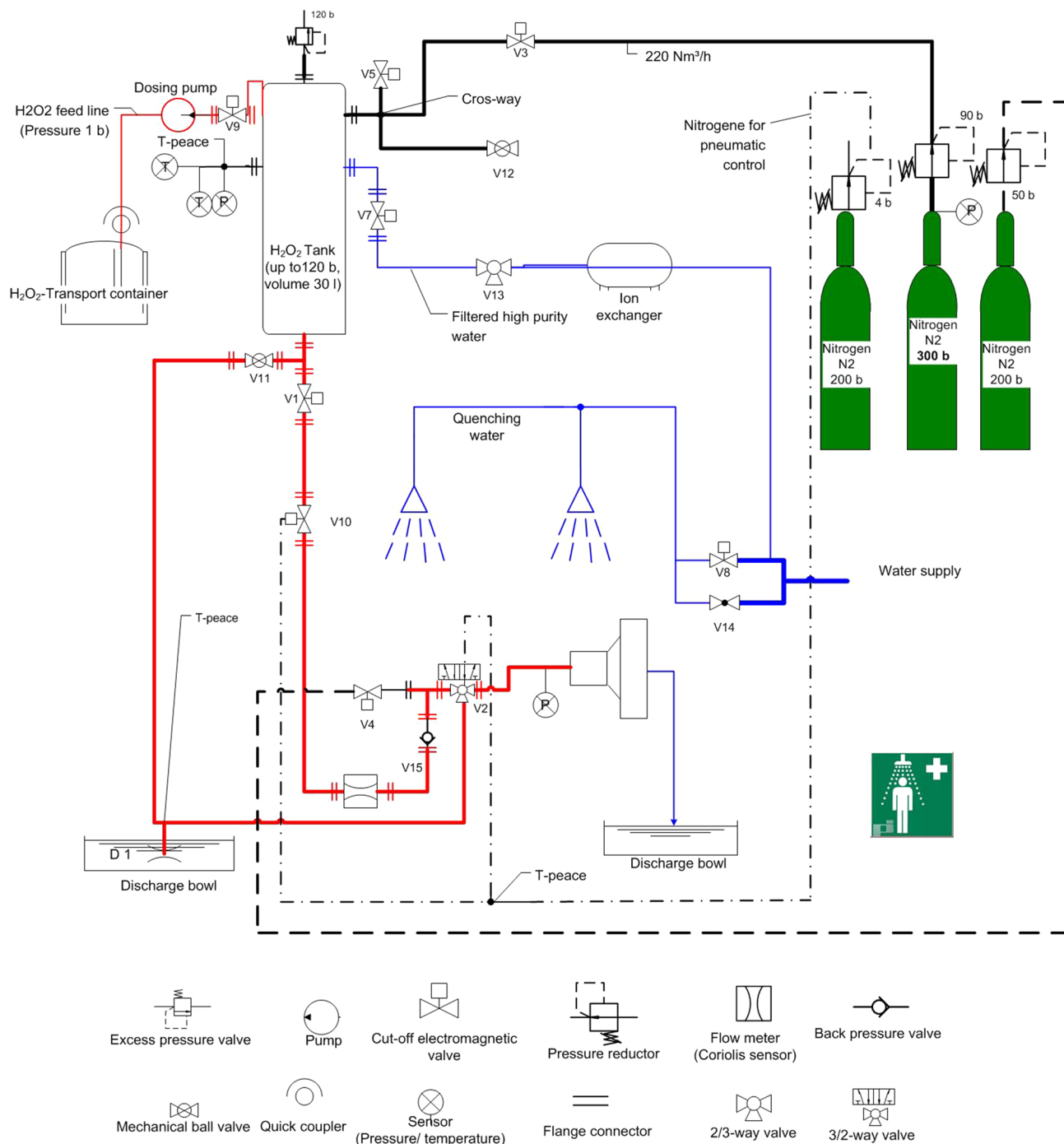


Fig. 6 H₂O₂—flowchart (HRE test bed)

On one of the lateral connection a solenoid valve (V9) is attached, which in the open state allows the charging of the tank by means of a volumetric dosing pump. On the second lateral connection, a multi-branched manifold (pipe crossing) is mounted to connect one further solenoid

valve for pressure discharge (V5), one mechanical ball valve for manual emergency pressure blow off (V12), as well as one solenoid valve for tank pressurization with nitrogen up to 100 bar (V3). The necessary nitrogen flow of 0.33 m³/s for the tank supply is assured using a battery

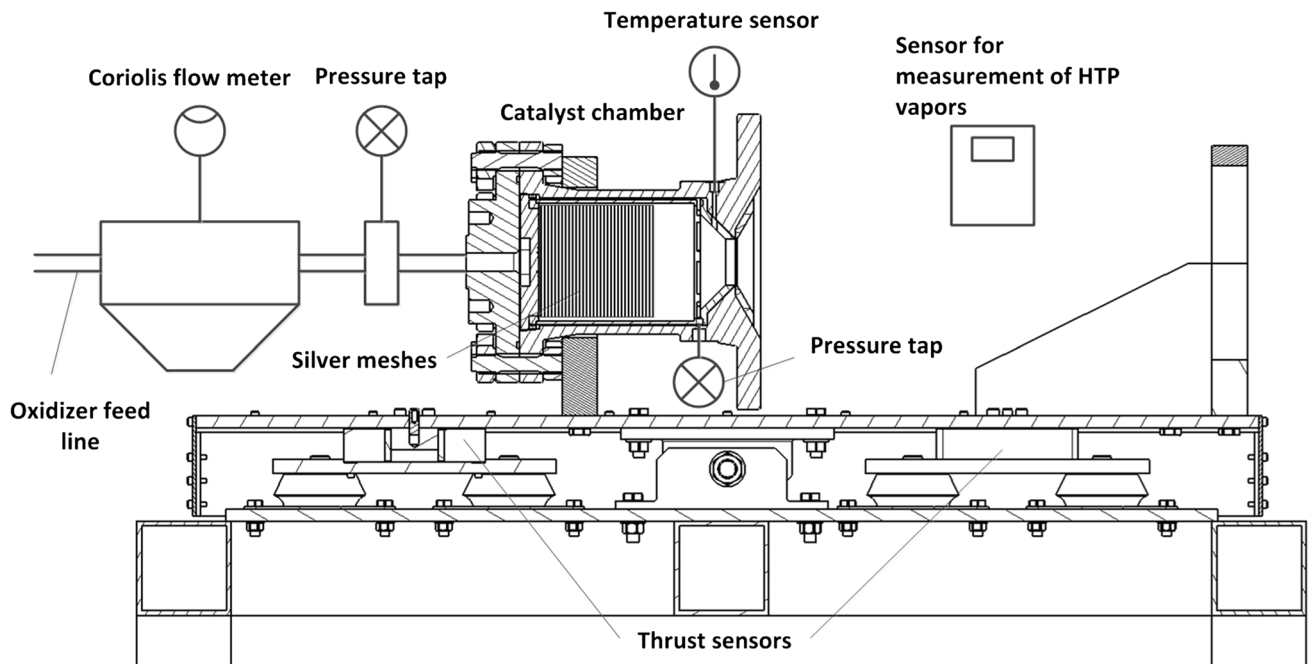


Fig. 7 Arrangement for testing of the HTP catalytic chamber

of nitrogen bottles with 300 bars. The system pressure can be adjusted by means of a dome pressure regulator and a pressure controller.

On the third lateral tank connection one further solenoid valve (V7) is attached, which enables flushing and purging of the tank and the feed system with high purity water before and after the tests. The permanent supply of filtered high purity water (on demand) is assured by one ion exchanger. The ion exchanger is connected to the water supply grid. The manually controlled ball valve (V13) allows the extraction of high purity water for cleaning of the transport canister, the catalyst chamber and the hybrid rocket engine parts after the tests. On the fourth flange connector, a T-fitting is fixed for housing two thermocouples and one pressure sensor for the supervision of the HTP pressure vessel. An excess pressure valve is attached on the tank cover plate, which opens at pressures higher than 120 bars to prevent tank from bursting. Safety tests show that the tank can withstand pressure loads up to 180 bars without stress or deformation overloads. The tank base includes the operation port for HTP extraction. On the port flange a T-fitting is mounted, which enables attachment of a manually controlled discharge valve (V11) and a solenoid valve (V1) which permits HTP feeding in open state in direction of the catalyst chamber. In emergency cases, the discharge valve (V11) enables the HTP to be directed over one specially designed high-pressure discharge nozzle (D1) in the dump basin.

At the main pipeline for HTP feeding between the valve (V1) and the catalyst chamber several control elements and

measurement sensors and instruments are attached. Behind the valve (V1) in the pipeline a pneumatically driven control valve (V10), a Coriolis flow meter, a check valve (V15), and a 3/2-way valve (V2) are installed. The combination of the control valve (V10) and the Coriolis sensor enable a precision HTP flow setting. The check valve (V15) prevents pressure shock spreading from the catalyst/engine chamber in the direction of the feed line and tank. Between the valves (V15) and (V2), a T-fitting is attached. On its third free connection, a solenoid valve (V4) is installed. In the open state, the valve (V4) enables feeding nitrogen with a pressure of 50 bar into the catalyst or engine chamber, and thus drying or clean-up of catalytic chamber or extinction of the HRE combustion chamber (if attached). After completion of the test, the valve (V2) guides the flow in the direction of the dump basin. This enables the system to be cleaned of accumulated waste HTP. All solenoid valves, which are in direct contact to the HTP, are of the coaxial type.

5 Applied measurement technique

Two pressure sensors are connected to the oxidizer feed line, one in front of the catalytic chamber and one at the catalytic chamber housing—in front of truncated outlet cone (s. Fig. 7). The difference of these two pressure values equals the pressure loss across the catalyst chamber. Both pressure sensors (KTE6000), delivered from

“Sensortech”, are of the membrane type and have a measurement range of 0–150 and 0–100 bar, respectively. The temperature of liquid HTP is measured within test plant tank. It was estimated that during HTP flowing inside of the feeding line up to the catalyst chamber injector, the fluid will be not additionally heated. This conclusion based on our temperature measurements inside feed line carried within some former experiments. Downstream of the catalyst bed (inside of the chamber truncated outlet cone), a shielded thermocouple of type N with a measurement range of 1200 °C is attached. In the catalyst chamber only one temperature of HTP decomposition products is measured. The position of unprotected thermocouple junction point is on the position $d/3$ in the radial direction, measured from the cone wall in direction to longitudinal chamber axis. Thereby, the measured temperature point is in the core flow of decomposed products and the influence of boundary layer is avoided. Despite of the fact that the catalytic chamber has no classic convergent-divergent nozzle, but rather a truncated subsonic cone on the exit, it was possible to measure the thrust force on the test bed. With a system of four photo and video cameras, the form and length of the exhaust steam/oxygen jet are optically registered. The concentration of hydrogen peroxide vapor is measured in the ambient air with a HTP gas detector of type Dräger X-am 5100 with the sensor XS H₂O₂ for a measurement range of 0–20 ppm. The named sensor for measurement of H₂O₂ vapor immission is fixed on the test bench close to the outlet of the catalyst chamber and observed with a camera. During all described tests the “alarm”, which starts by immission higher than 20 ppm, was not activated.

Concentration of liquid HTP is controlled indirectly by density measurement. The temperature of liquid HTP before the inflow in the catalyst chamber is also measured with type J thermocouple. The HTP mass flow measurement is realized with the Coriolis flow meter OPTIMASS 8000 obtained from KROHNE (configured measurement range 0–1.5 kg/s HTP).

6 Preliminary test results

The presented preliminary results were attained during a measurement campaign carried out at the DLR test range Trauen (s. Fig. 8) in July 2013. Five experiments were successfully conducted and post-analysis and evaluation were done. Emission of HTP vapor outside the catalyst chamber during all experiments was not observed and it can be concluded that the decomposition process was finished. Evaluation of the HTP catalyst chamber efficiency is carried out by means of the characteristic velocity efficiency η_{c^*} and the temperature efficiency $\eta_{\Delta T}$. The characteristic velocity efficiency is an important criterion for estimating



Fig. 8 Test facility for hybrid rocket engines at DLR Trauen, Fassberg, Germany

the energetic efficiency of the catalytic chamber. It can be given with the following expression:

$$\eta_{c^*} = \frac{c_{\text{exp}}^*}{c_{\text{theo}}^*} \quad (3)$$

The experimental value of characteristic velocity c_{exp}^* is determined with the expression:

$$c_{\text{exp}}^* = \frac{\sqrt{R_i \cdot T_{\text{exp}}}}{\Gamma} \quad (4)$$

In Eq. (4), T_{exp} is the measured temperature of the decomposed gas mixture behind the catalyst bed in the catalyst chamber. In gas dynamic theory, the value Γ is known as the Vandekerckhove function:

$$\Gamma = \sqrt{\kappa} \left(\frac{2}{\kappa + 1} \right)^{\frac{\kappa+1}{2(\kappa-1)}} \quad (5)$$

The catalyst bed is well isolated from the housing by means of a gap between the housing and the catalyst mount (s. Fig. 5). Due to this fact, the polytropic constant $n = (c_p/c_v)_{\text{diabatic}}$ in the first approximation can be taken as equal to the ratio κ and can be used for calculation of expressions (4) and (5). The alternative calculation of c_{exp}^* using the equation

$$c_{\text{exp}}^* = p_{c,\text{exp}} \cdot \frac{A_t}{\dot{m}_{\text{exp}}} \quad (6)$$

Table 1 Estimated efficiency of the catalyst chamber during carried out tests

	Test 1	Test 2	Test 3	Test 4	Test 5
Mass flow—measured \dot{m}_{exp} [kg/s]	0.702	0.745	1.037	1.01	0.994
Process time τ [s]	6.6	10.8	5.4	3.5	3.2
Mean char. velocity $c_{\text{exp,mean}}^*$ [m/s]	845.93	870.16	894.45	858.41	879.89
Max char. velocity $c_{\text{exp,max}}^*$ [m/s]	894.74	895.78	895.23	858.41	879.89
Chamber pressure p_c [bar]	4.82	5.24	7.51	7.64	7.46
Mean temperature efficiency $\eta_{\Delta T, \text{mean}}$ [%]	79.05	86.22	93.61	82.72	89.15
Max. temperature efficiency $\eta_{\Delta T, \text{max}}$ [%]	93.74	94.01	93.88	82.72	89.15
Mean char. vel. efficiency $\eta_{c^*, \text{mean}}$ [%]	92.46	95.1	97.76	93.82	96.17
Max. char. vel. efficiency $\eta_{c^*, \text{max}}$ [%]	97.81	97.9	97.85	93.82	96.17
Total pressure drop across the catalyst bed, Δp_{CB} [bar]	7.45	9.63	12.9	13.16	12.64
	5.5	6.52			
Pressure drop across feed line, Δp_{FL} [bar]	85.0	81.4	76.7	76.18	77.0
	88.6	86.8			

is not suitable, because the applied catalyst chamber has no convergent–divergent nozzle on the exit, as it is usual for monopropellant HTP rocket engines. The flow conditions within the catalyst chamber in vicinity of measurement sensors do not correspond well with the throat conditions in a nozzle. The theoretical values of decomposition temperature T_{ad} and c_{theo}^* are determined with the Gordon-McBride CEA2 thermochemistry code [11]. In the code, the relationships between named variables are also based on the formulation:

$$c_{\text{theo}}^* = \frac{\sqrt{R_i \cdot T_{\text{ad}}}}{\Gamma} \quad (7)$$

For the HTP PROPULSE 875 (Evonik, Deutschland) with a H_2O_2 concentration of 87.5 wt%, the adiabatic decomposition temperature is $T_{\text{ad}} = 968.46$ K and the theoretical characteristic velocity is $c_{\text{theo}}^* = 913$ m/s. With the CEA code, the calculated values for T_{ad} and c_{theo}^* do not show any change with pressure increase, but in reality discrepancies of few percent, dependent of pressure level in the chamber, are possible [12]. The measured temperature T_{exp} , as well as the corresponding value c_{exp}^* are lower (s. Table 1) than the calculated theoretical values. This can be explained with the losses due to the cooling in the injector and the chamber head area downstream the catalyst bed and the discrepancy between ideal 1D-expansion/real expansion of decomposed gas products in the convergent injector cone. One additional indicator for estimating the efficiency of the catalytic chamber is the temperature efficiency

$$\eta_{\Delta T} = \frac{T_{\text{exp}} - T_{\text{env}}}{T_{\text{ad}} - T_{\text{env}}} \quad (8)$$

The two further important operational criteria for characterisation of a catalytic chamber are the pressure drop across the catalyst bed Δp_{CB} and the total pressure drop

across the feed line Δp_{FL} (between oxidizer tank and injector on HRE combustor head). They have important influence on decomposition process stability and structure weight (catalyst chamber and whole oxidizer feeding system).

The results of the measured efficiency criterions are given in Table 1. The mean temperature efficiency $\eta_{\Delta T, \text{mean}}$ is in the range of 79.5–93.6 %. Maximum temperature efficiency $\eta_{\Delta T, \text{max}}$ is in the range of 82.72–94 %. During all tests, the mean characteristic velocity efficiency $\eta_{c^*, \text{mean}}$ exceeds 92 % and maximum characteristic velocity efficiency $\eta_{c^*, \text{max}}$ is approximately 98 %. The high-pressure drop across the feed line is a result of the of control valve V10 (s. Fig. 6). This valve controls the mass flow and therefore it generates a pressure drop. The pressure within the tank is constant for all tests to ensure constant pressure drop characteristics for the control valve and the mass flow sensor. All these parameters are realized by a mass flow load of the catalyst chamber in the range between 54 and 78 % of the designed capacity. The conducted tests and analysis indicate that for high loads of the catalyst chamber with a HTP mass flow of around 1.0 kg/s the process shows good efficiency.

The reported tests with the catalyst chamber are carried out in the transient and steady regime. By application of relatively high HTP mass flows, the transition from start point to steady state needs a period of up to 4 s. The same transition time is necessary to shut off the process from the moment when the control valve is closed. This is a consequence of accumulated HTP mass within the catalyst bed, which must be exhausted. The maximum mass flow achieved in the presented test results (s. Figs. 9, 10, 11, 12, 13) is an indicator for possible steady state flow. This conclusion should be confirmed by forthcoming long duration steady state tests with test times up to 30 s. The mean values of efficiency criteria during test 1 and test 4 are more

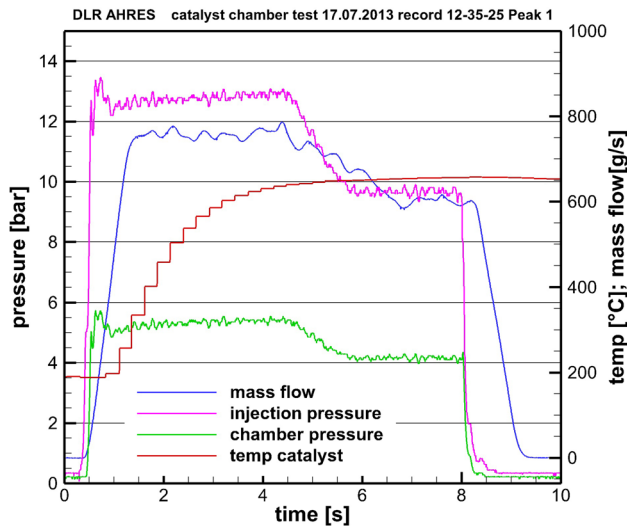


Fig. 9 H₂O₂ catalytic chamber test 1 (peak 1) with main mass flow 702.4 g/s

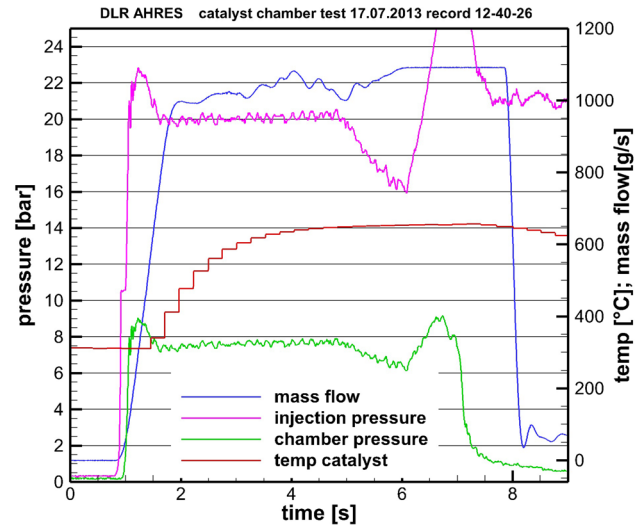


Fig. 11 H₂O₂ catalytic chamber test 3 with main mass flow 1037 g/s

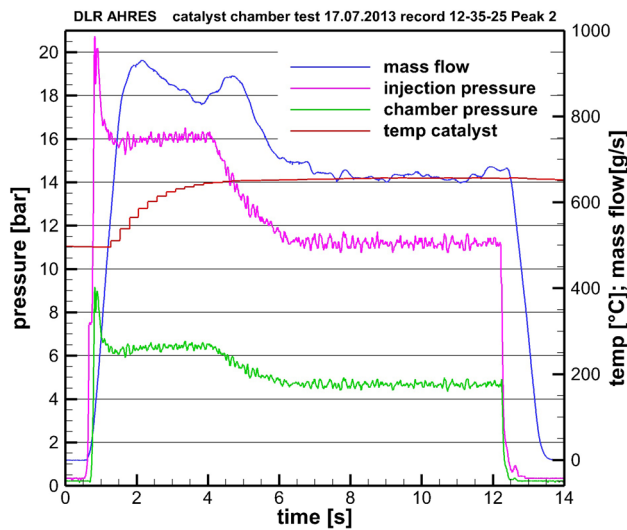


Fig. 10 H₂O₂ catalytic chamber test 2 (peak 2) with main mass flow 745.2 g/s

representative for the catalyst chamber under transient working conditions. Tests 2, 3 and 5 could be regarded as quasi stationary.

The properties of the exhaust jets (s. Figs. 14, 15) are dependent on the mass flow value. At lower mass flows (generally under 120 g/s) exhaust jets cool faster and saturated water steam will be generated. That makes the jet clearly visible and non-transparent. For higher mass flows, the exhaust jet comprises sufficient energy to deliver water steam in overheated condition and the jet remains transparent and rarely visible. During tests in mass flow range between 700 and 1037 g/s the jet is fully transparent.

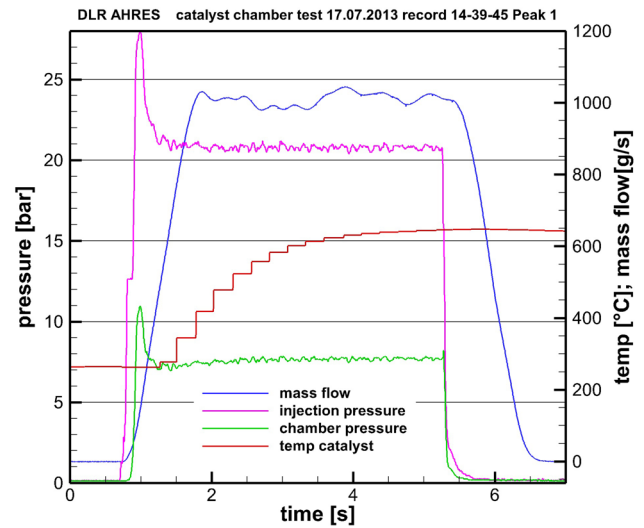


Fig. 12 H₂O₂ catalytic chamber test 4 with main mass flow 1010 g/s

Figures 11 and 13 show two experiments, where strong pressure peaks occur at the end of the experiments. The pressure peaks are an effect of the shutdown behavior of the control valve V10. The diagrams on Figs. 9, 10, 11, 12 and 13 and Table 2 show the appearance of low frequency instabilities with frequencies between 8.8 and 13.6 Hz and amplitudes between 0.4 and 1.3 bars during the tests. The measured amplitudes are low and can be regarded more as hydraulic roughness than as instabilities. The driving force due to coupling between feed system and vaporization delay also has some influence on instabilities during decomposition in the catalyst chamber. The degree of influence due to this coupling cannot be estimated without further and more detailed tests.

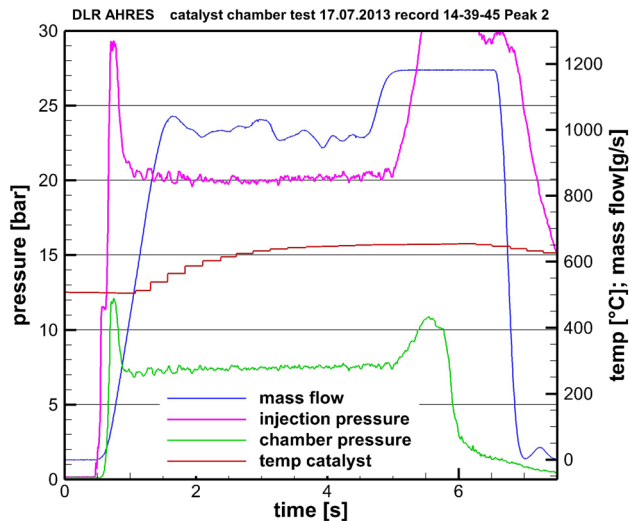


Fig. 13 H_2O_2 catalytic chamber test 5 with main mass flow 993.83 g/s



Fig. 14 Test with H_2O_2 catalyst chamber carried out in March 2013 (mass flow 120 g/s)

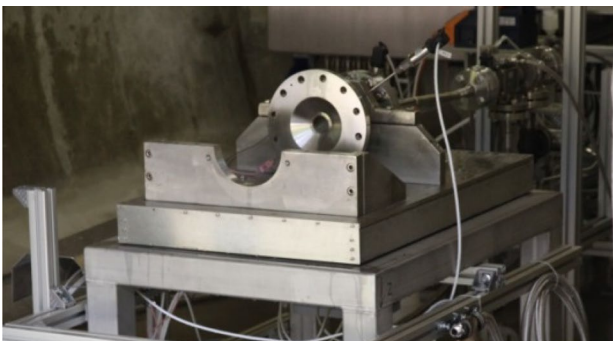


Fig. 15 Test with H_2O_2 catalyst chamber carried out in July 2013 (mass flow 745 g/s)

Table 2 Properties of low frequency instabilities within catalyst chamber during tests

	Test 1	Test 2	Test 3	Test 4	Test 5
Mass flow—measured \dot{m}_{exp} (kg/s)	0.702	0.745	1.037	1.01	0.994
Chamber pressure p_c (bar)	4.82	5.24	7.51	7.64	7.46
Frequency (Hz)	8.79	6.76	8.51	10.86	13.64
Total amplitude (bar)	0.3815	0.6378	1.31	0.38	0.57
Positive amplitude (bar)	0.1299	0.3113	1.5677	0.0144	0.1931
Negative amplitude (bar)	0.2516	0.3265	NA	0.3731	0.3837

7 Conclusions

The conducted tests confirm the design functionality and flexibility of the catalyst chamber. In addition, design requirements (e.g., HTP steady mass flow up to 1000 g/s, complete decomposition of HTP to water steam and oxygen without remaining hydrogen peroxide vapors, ignition temperature for HTPB exceeded) are achieved. An activated silver mesh catalyst pack operates well with HTP PROPULSE 875. The decomposition temperature was approximately 300 °C below the melting point of silver. Furthermore, silver is cheap compared to platinum and is known for good commercial availability.

In this paper, the preliminary results of a test campaign, carried out in summer 2013, are presented, with the goal to estimate the properties and the thermal efficiency of the catalyst chamber for a HRE developed within the DLR AHRES research program. Further tests with higher mass flow up to 1200 g/s under steady conditions are in preparation. The instabilities within catalyst chamber and HRE combustion chamber observed in earlier tests, carried out in March 2013, are eliminated successfully due to modification of chamber construction. The achieved characteristic velocity efficiency is satisfying, but it is expected that it will rise under steady state working conditions

References

- Božić, O., Pormann, D., Lancelle, D., Hartwig, A.: Program AHRES and its contribution to assess features and current limitations of hybrid rocket propulsion. 63th Congress of International Astronautical Federation, IAC-12-C4. 2.8 (2012)
- May, S., Lancelle, D., Pormann, D.: Mathematical modeling of a high test peroxide catalyst chamber for hybrid rocket engines. 13th ONERA-DLR aerospace symposium (2013)
- Pirault-Roy, L., Kappenstein, C., Guérin, M., Eloirdi, R., Pillet, N.: Hydrogen peroxide decomposition on various supported catalysts effect of stabilizers. *J. Propuls. Power.* **18**(6), 1235–1241 (2002)

4. Joksimović-Tjapkin, S.M., Delić, D.: Kinetics of concentrated hydrogen peroxide decomposition on a rotating disk. *Ind. Eng. Chem. Fundam.* **12**(1), 33–39 (1973)
5. Lim, H., An, S., Kwon, S., Rang, S.: Hydrogen peroxide gas generator with dual catalytic beds for nonpreheating startup. *J. Propuls. Power.* **23**(5), 1147–1151 (2007)
6. Romeo, L., Torre, L., Pasini, A., d'Agostino, L., Caldarezzo, F.: Comparative characterization of advanced catalytic beds for hydrogen peroxide thrusters. *AIAA, Paper 2008-5027* (2008)
7. Yang, H., Zhang, T., Tian, H., Tang, J., Xu, D., Yang, W., Lin, L.: Effect of Sr substitution on catalytic activity of $\text{La}_{1-x}\text{Sr}_x\text{MnO}_3$ ($0 < x < 0.8$) perovskite-type oxides for catalytic decomposition of hydrogen peroxide. *React. Kinet. Catal. Lett.* **73**(2), 311–316 (2001)
8. Torre, L., Pasini, A., Romeo, L., d'Agostino, L.: Firing performance of advanced hydrogen peroxide catalytic beds in a monopropellant thruster prototype. *44th AIAA/ASME/SAE/ASEE joint propulsion conference and exhibit, AIAA 2008-4932* (2008)
9. Jonker, W. A., Mayer, A. E. H. J., Zandbergen, B. T. C.: Development of a rocket engine igniter using the catalytic decomposition of hydrogen peroxide. *3rd ESA international conference on green propellants for space propulsion, SP-635* (2006)
10. Neumaier, W. W. Jr., Wells, M., Brinkley, A., Talty, T.: Development of a 90% hydrogen peroxide mono-propellant propulsion system for the warm gas test article. *48th AIAA/ASME/SAE/ASEE joint propulsion conference and exhibit, AIAA 2012-3755* (2012)
11. Gordon, S., McBride, B. J.: NASA—GLENN chemical equilibrium program CEA2. (2004); Refs: NASA RP-1311-Part 1 (1994) and NASA RP-1311-Part 2 (1996)
12. Walsh, R. F., Sutton, A. M.: Pressure effects on hydrogen peroxide decomposition temperature. *5th Int'l hydrogen peroxide propulsion conference, AFRL-PR-ED-TP-2002-203* (2002)
13. Božić O., Lancelle, D. M., May, S., Porman, D.: Experimental evaluation of a high test peroxide catalyst chamber for a hybrid rocket engine, *5th European conference for aeronautics and space sciences (EUCASS), Munich, Germany, 1–5 July 2013*
14. Peroxide propulsion. <http://www.peroxidepropulsion.com/>. Accessed 29 July 2015